Electronic Supplementary Material (ESI) for Dalton Transactions.

Modulation of aggregation of human prion protein $PrP_{106-126}$ by indole based cyclometallated palladium complex

Rahul Chauhan,[a] Govinda R. Navale,[a] Saakshi Saini,[b] Abhishek Panwar,[c] Prashant,[a] Rajat Saini,[a] Partha Roy,[b] Kaushik Ghosh[a,b*]

[a.] *Department of Chemistry, Indian Institute of Technology, Roorkee- 247667, Uttarakhand*
[b.] *Department of Biosciences and Bioengineering, Indian Institute of Technology, Roorkee-247667, Uttarakhand*
[c.] *Department of Chemistry, National Institute of Technology Manipur, Langol-795004*

*To whom correspondence should be addressed.

E-mail: kaushik.ghosh@cy.iitr.ac.in

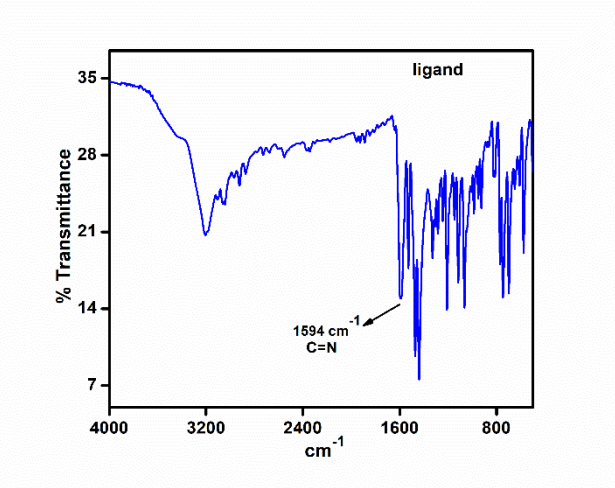

Figure S1. FT-IR spectrum of Ligand.

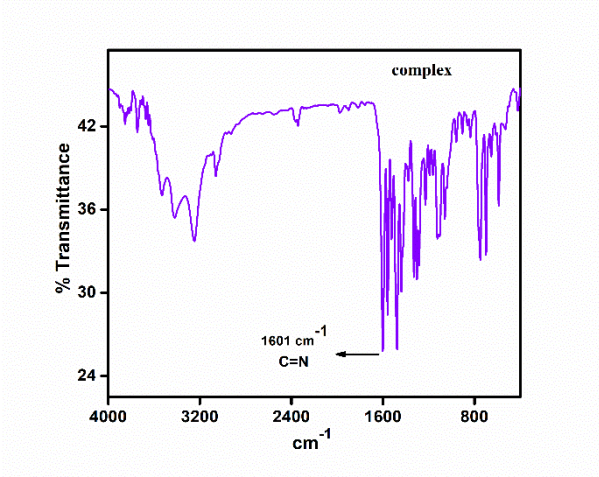

Figure S2. FT-IR spectrum of complex.

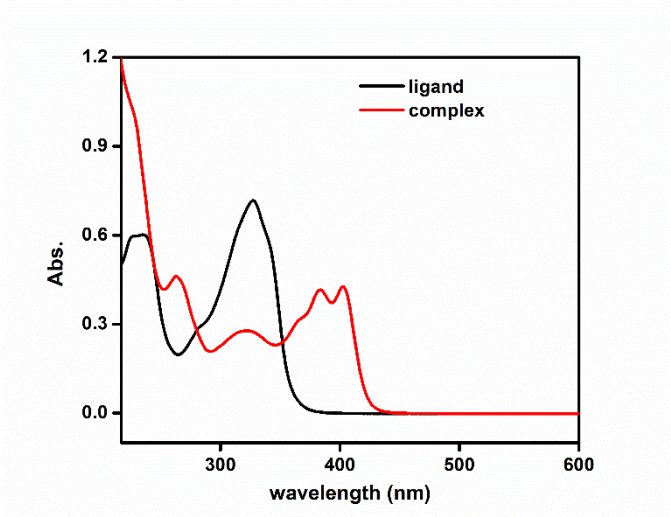

Figure S3. UV-Visible spectra of ligand (25.6 µM) and complex (23 µM) in CH_3CN.

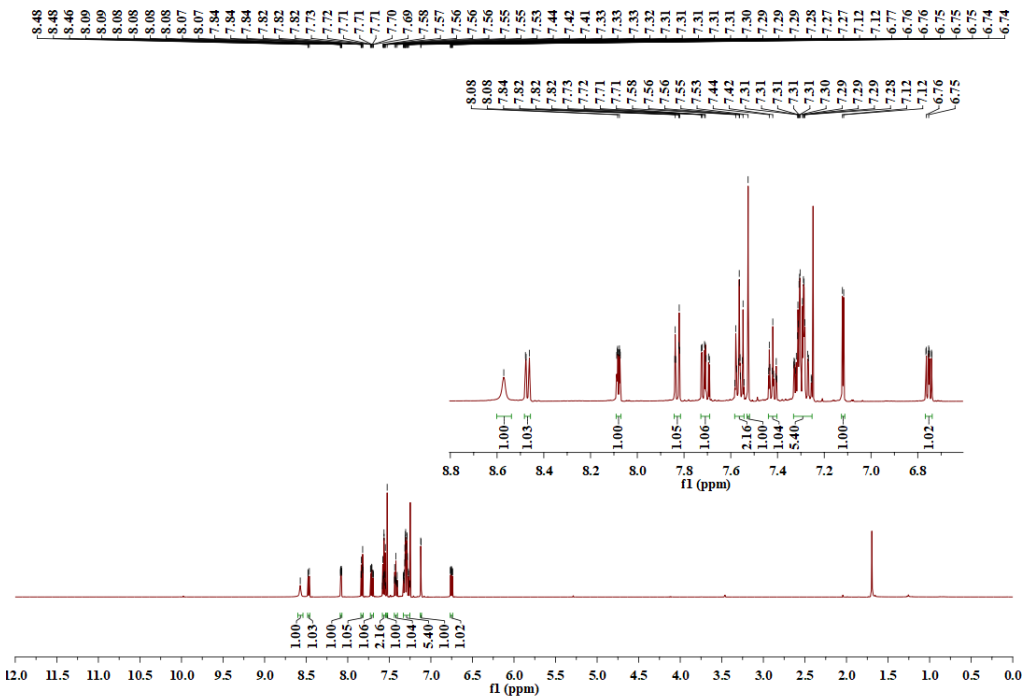

Figure S4: ^{1}H NMR spectra of Ligand in $CDCl_3$**.**

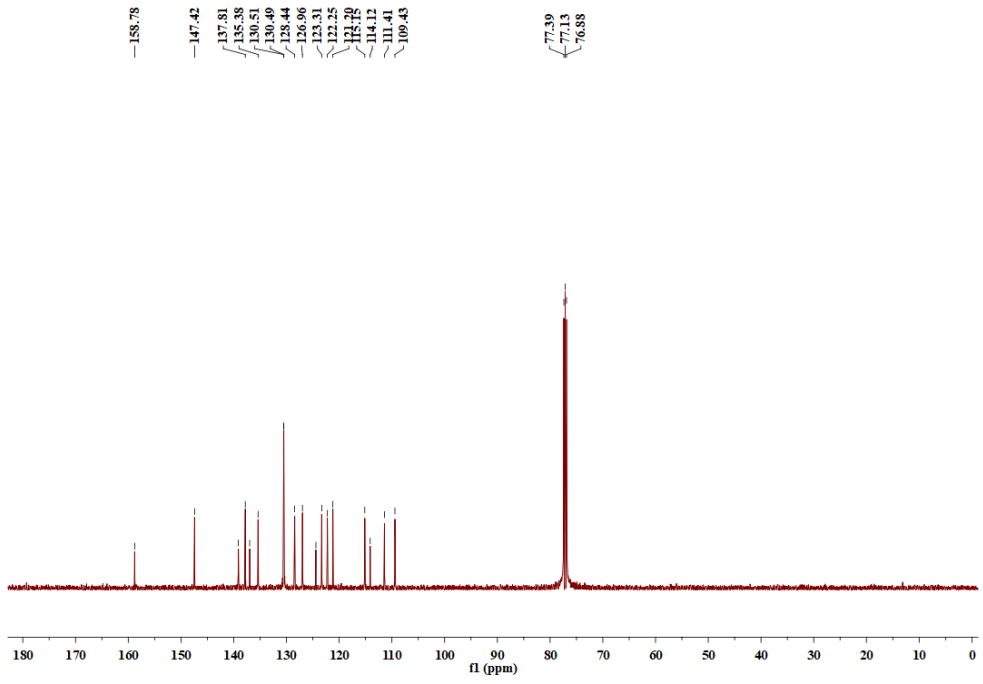

Figure S5: ^{13}C NMR spectra of Ligand in $CDCl_3$.

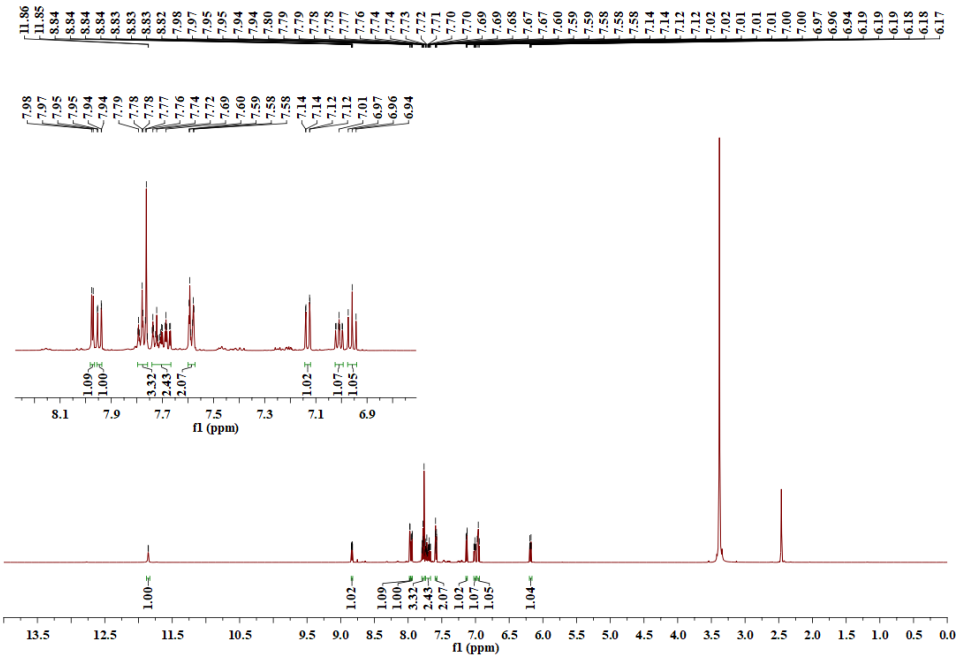

Figure S6: ^{1}H NMR spectra of complex in DMSO-d_6.

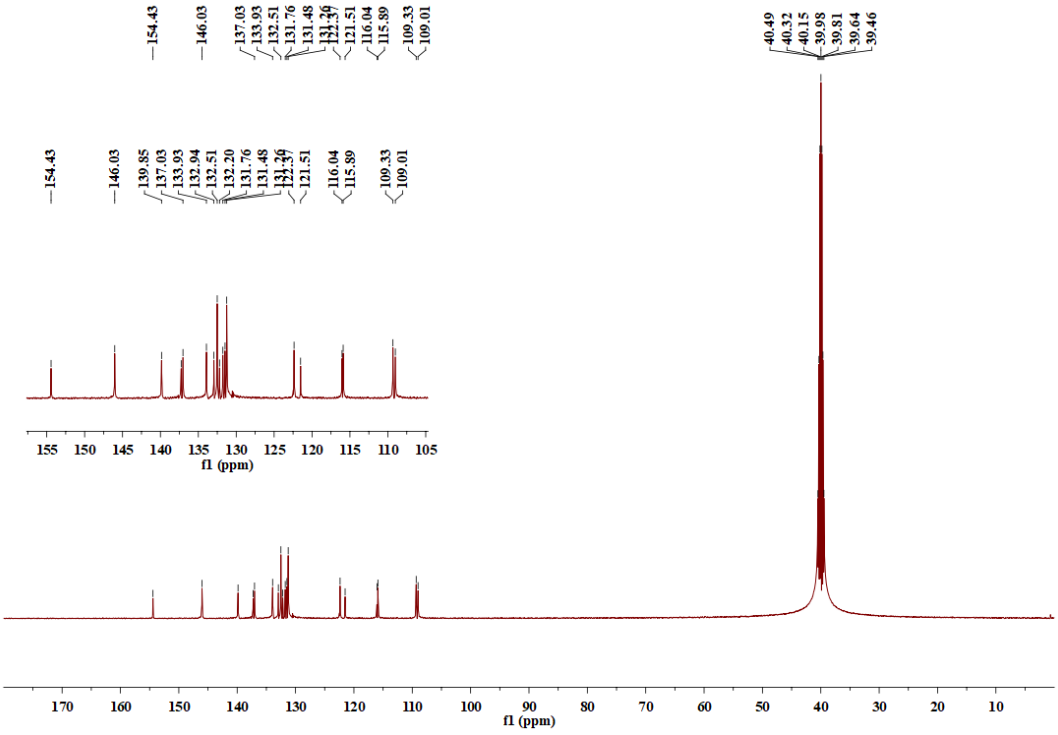

Figure S7: ^{13}C NMR spectra of complex in DMSO-d_6.

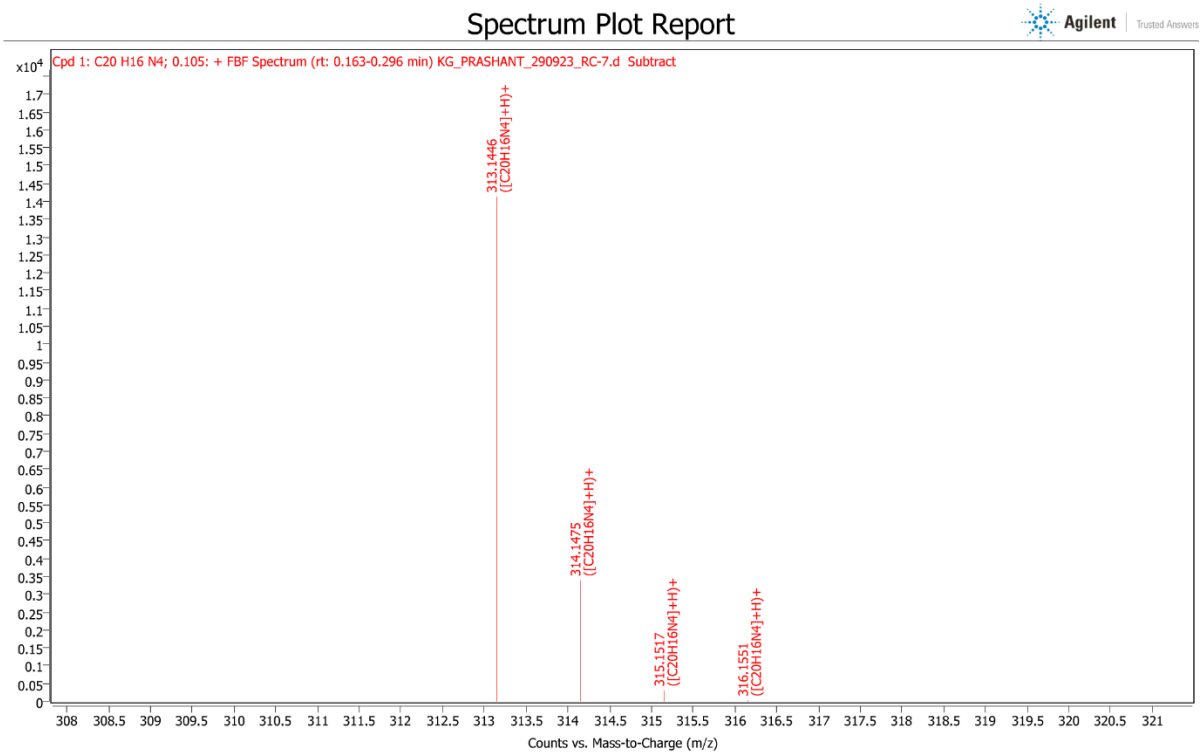

Figure S8: HR-MS spectrum of Ligand.

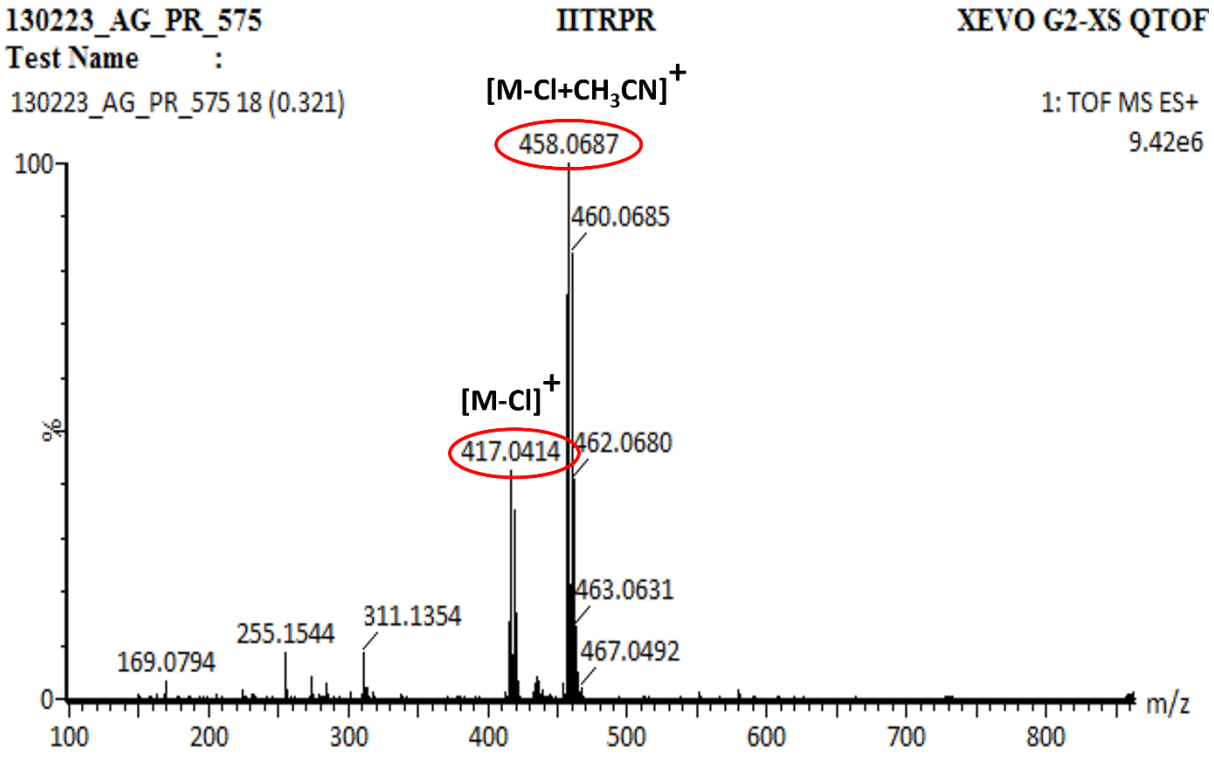

Figure S9: HR-MS spectra of complex.

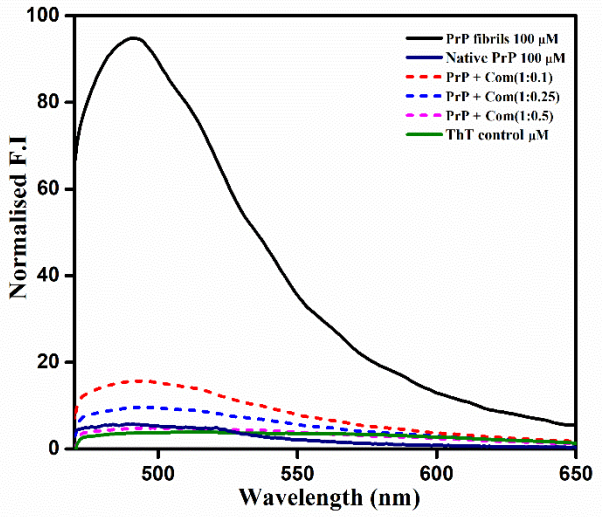

Figure S10: End point measurements of native $PrP_{106-126}$ (0 h), $PrP_{106-126}$ fibrils (24 h) and with complex at different concentrations measured by ThT fluorescence after incubation for 24 h at 37º C. Conditions: All experiments were conducted at physiological pH in PBS buffer, [$PrP_{106-126}$]=100 µM, [ThT]= 10 µM and [complex]= 10, 25 and 50 µM.

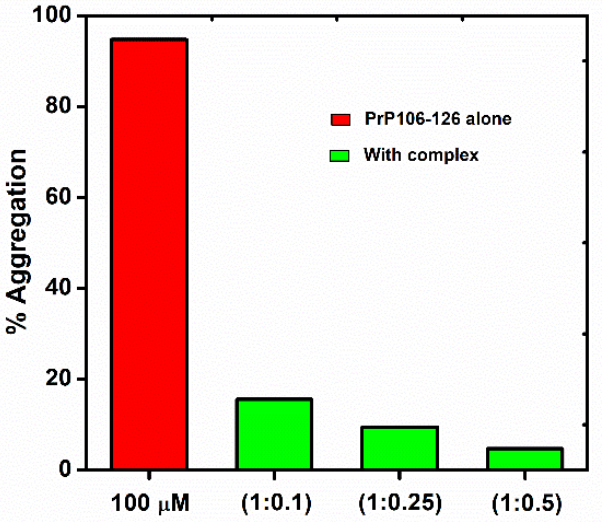

Figure S11: Bar diagram of ThT fluorescence showing the amount of aggregation in the absence and presence of complex at varying concentration after incubation for 24 hours at 37º C

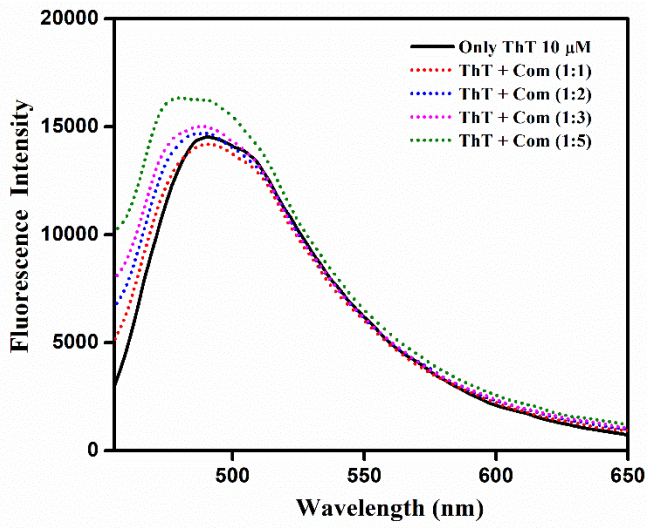

Figure S12. The ThT spectra carried out in the presence and absence of complex at different concentration. The FL intensity of metal complex is small enough to be ignored as compared with fluorescence intensity of $PrP_{106-126}$. Conditions: λ_{ex} – 440 nm, λ_{emm}- 482-485 nm, PBS Buffer 10 mM of pH 7.4, [ThT]- 10 µM and [complex]- 10, 20, 30, and 50 µM.

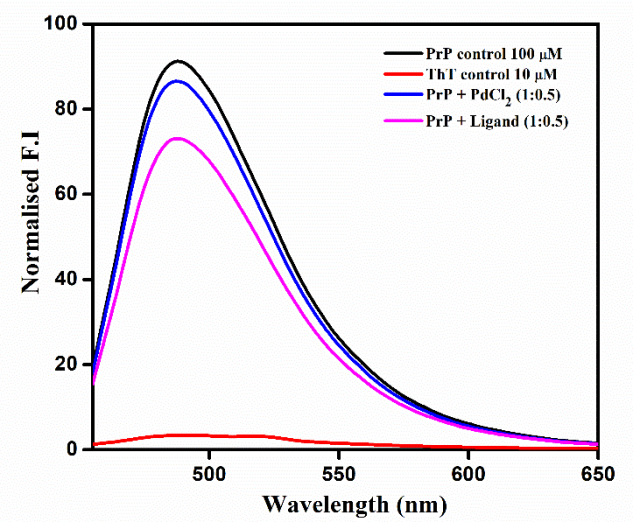

Figure S13: ThT fluorescence assay of free $PrP_{106-126}$ and in presence of ligand and $PdCl_2$ after incubated for 24 hours at 37° C. Conditions: Conditions: λ_{ex} – 440 nm, λ_{emm}- 482-485 nm, PBS buffer 10 mM of pH 7.4, [$PrP_{106-126}$]- 100 µM, [ThT]- 10 µM and [Ligand]/[$PdCl_2$]- 50 µM.

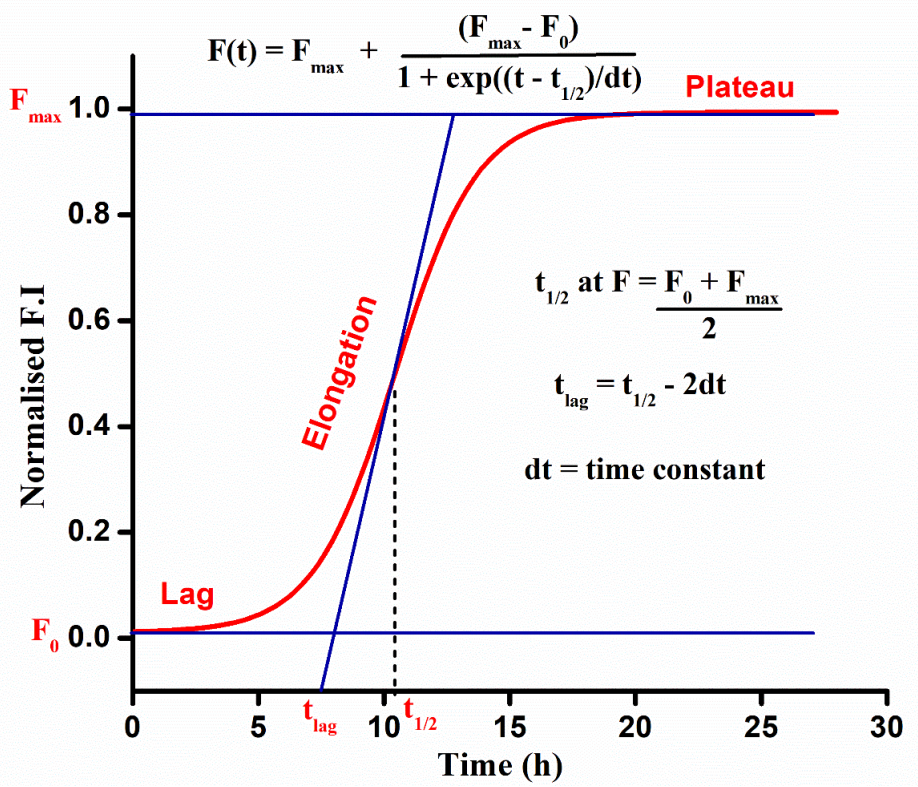

Figure S14: The Boltzmann sigmoidal curve and equation for calculation of time parameters. Horizontal blue lines indicate the lowest and highest normalised fluorescence intensity. The red line is a Boltzmann sigmoidal equation fit (with a blue tangent line at the intermediate value of the fit). The intercept of tangent line at x- axis gives t_{lag} (lag time) whereas dashed line perpendicular to x-axis at intermediate value of fit gives half time, $t_{1/2}$.

Histidine Binding assay

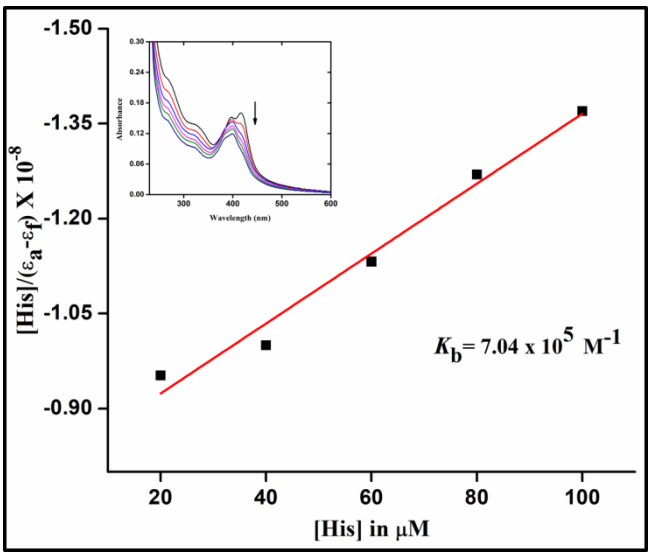

Figure S15: Histidine binding assay of complex using UV-Visible spectroscopy.

Methionine Binding assay

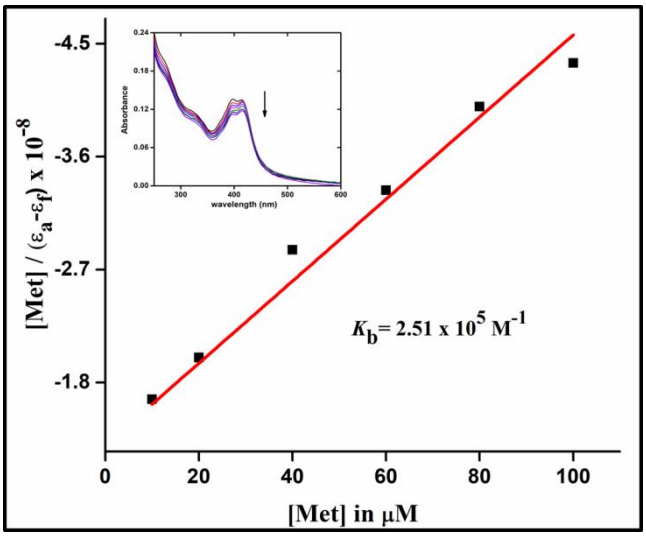

Figure S16: Methionine binding assay of complex using UV-Visible spectroscopy.

Procedure for amino acid binding assay:

Absorption spectra of complex at 10 μM concentration upon addition of histidine and methionine (0-100 μM) with incubation of 3-5 minutes at every concentration. The (↓) arrows indicate absorbance changes upon increasing the amino acid (A.A) concentration. The amino acid binding constant (K_b) for complex is plotted as [A. A]/($\varepsilon_a - \varepsilon_f$) vs [A. A]. The data were applied to the following equation, and the binding constant K_b was calculated using the wolfe-shimmer equation similar to that of DNA binding assay,

$$[A.\ A]/[\varepsilon_a-\varepsilon_f] = [A.\ A] / [\varepsilon_b-\varepsilon_f] + 1/K_b[\varepsilon_b-\varepsilon_f]$$

Where [A. A] is the concentration of amino acid in μM, ε_a is the extinction coefficient of the complex at a given amino acid concentration, ε_f is the extinction coefficient of the complex in free solution, and ε_b is the extinction coefficient of the complex when fully bound to amino acid. A plot of [A. A]/[ε_a-ε_f] versus [A. A] gave a slope and intercept equal to 1/[ε_b-ε_f] and (1/K_b) [ε_b-ε_f], respectively. The intrinsic binding constant K_b is the ratio of the slope to the intercept.

$PrP_{106-126}$ Binding assay

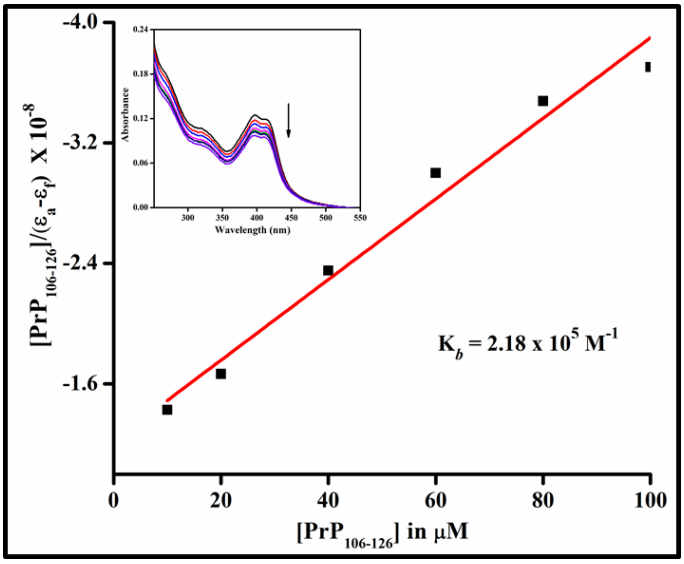

Figure S17: $PrP_{106-126}$ binding of complex using electronic absorption spectroscopy in PBS buffer in physiological pH.

Procedure:

Similar to His and Met binding assay.

DNA Binding Assay

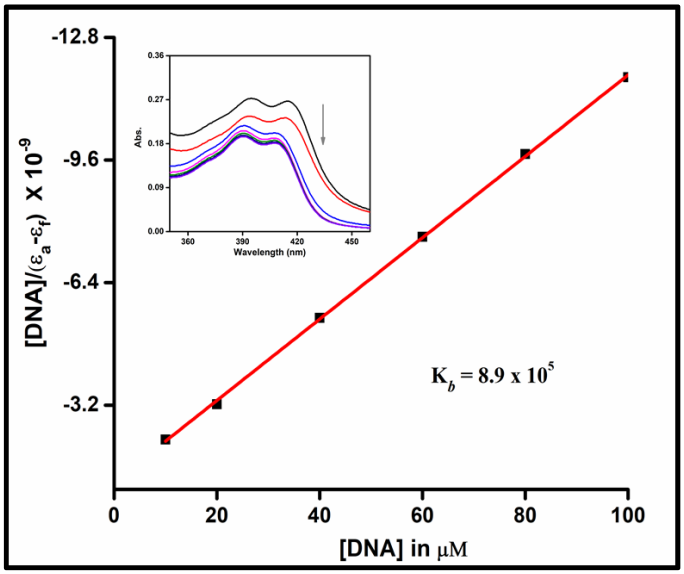

Figure S18: DNA binding of complex using electronic absorption spectroscopy.

Procedure:

All titrations were carried out in Tris buffer (pH 7.2). The DNA concentration per nucleotide was determined by absorption spectroscopy using the molar absorption coefficient (6600 M^{-1} cm^{-1}) at 260 nm. A solution of CT-DNA gave a ratio of UV absorbance at 260 and 280 nm of 1.8–1.9, indicating that DNA was pure and free of protein. The absorption titration experiments of complex were performed at a fixed complex concentration (20 μM) until the absorbance did not change anymore with increasing DNA concentration (0–100 μM) with a incubation of 3-5 minutes at every concentration. The electronic absorption spectra were determined in the range 200–500 nm. The complex–DNA solutions were allowed to incubate for 5 min before the absorption spectra were recorded. The data were applied to the following equation, and the intrinsic binding constant K_b was calculated using the Wolfe-Shimmer equation:

$$[DNA]/[\varepsilon_a - \varepsilon_f] = [DNA]/[\varepsilon_b - \varepsilon_f] + 1/K_b[\varepsilon_b - \varepsilon_f]$$

Where [DNA] is the concentration of DNA in base pairs, ε_a is the extinction coefficient of the complex at a given DNA concentration, ε_f is the extinction coefficient of the complex in free solution, and ε_b is the extinction coefficient of the complex when fully bound to DNA. A plot of [DNA]/ [$\varepsilon_a - \varepsilon_f$] *versus* [DNA] gave a slope and intercept equal to 1/[$\varepsilon_b - \varepsilon_f$] and (1/$K_b$) [$\varepsilon_b - \varepsilon_f$], respectively. The intrinsic binding constant K_b is the ratio of the slope to the intercept.

Fluorescence Binding Assay

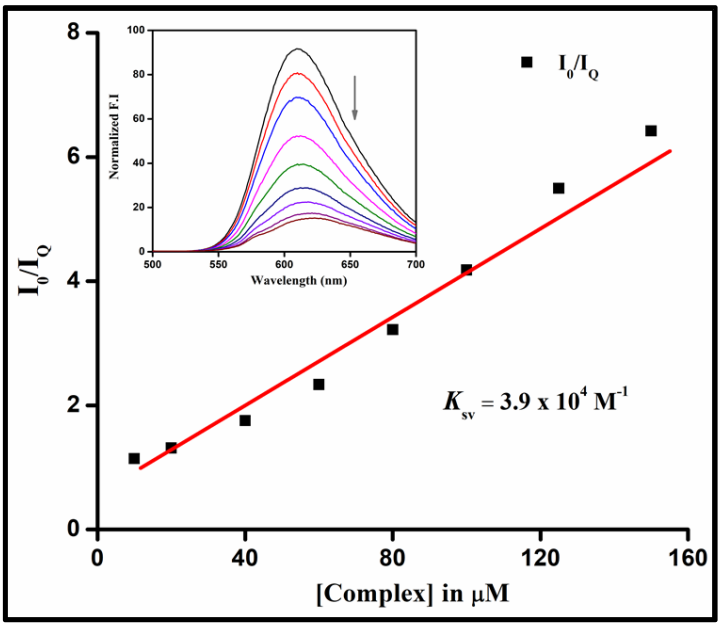

Figure S19: DNA binding assay of complex using fluorescence spectroscopy.

Procedure:

Fluorescence titration experiments were carried out to support the interaction between the complex and CT-DNA further. The fluorescence emission spectra of both the DNA (10 μM) + EtBr (5 μM) in the presence of various concentrations of the quencher complex (0–150 μM) in Tris–HCl buffer (pH 7.2) were recorded between 300 and 700 nm at room temperature with the excitation wavelength set at 285 nm. The Stern–Volmer equation was used to determine the mechanism of interaction:

$$I_0/I_{[Q]} = 1 + K_{SV}/[Q] \text{ or } K_{SV} = ((I_0/I_{[Q])} - 1)/[Q]$$

In this equation, I_0 and $I_{[Q]}$ are the fluorescence intensities in the absence and presence of the quencher (complex), K_{SV} is the Stern–Volmer quenching constant, and [Q] is the concentration of the quencher (complex). After plotting ($I_0/I_{[Q])}$ against [Q], the slope can be determined to give the value of K_{SV}, the Stern–Volmer constant.

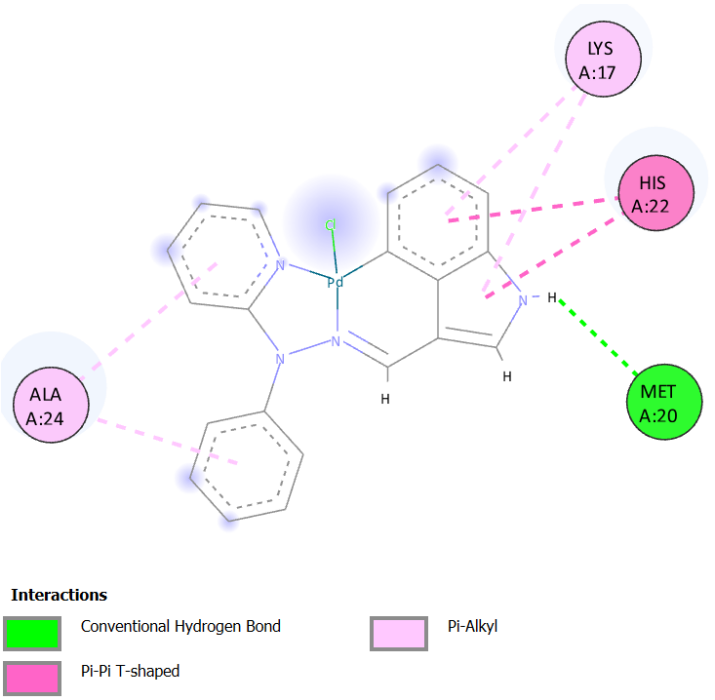

Figure S20: 2D Schematic representation displaying the most likely non-covalent interactions between complex and peptide

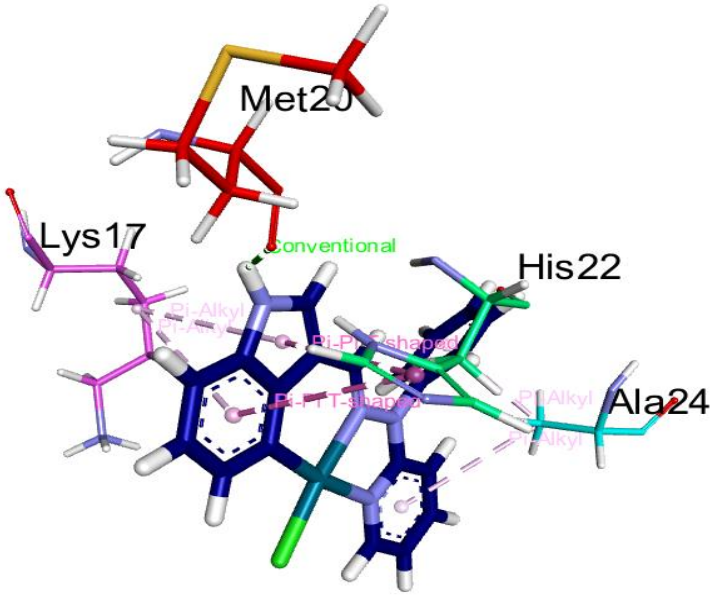

Figure S21: 3D Schematic representation displaying the type of non-covalent interaction between complex and peptide residues

	Name	Visible	Color	Parent	Distance	Category	Types	From	From Chemistry	To	To Chemistry
1	d:RES1:H41 - A:MET20:O	Yes		Ligand Non-...	2.0423	Hydrogen Bond	Conventional Hydrogen Bond	d:RES1:H41	H-Donor	A:MET2...	H-Acceptor
2	A:HIS22 - d:RES1	Yes		Ligand Non-...	4.81596	Hydrophobic	Pi-Pi T-shaped	A:HIS22	Pi-Orbitals	d:RES1	Pi-Orbitals
3	A:HIS22 - d:RES1	Yes		Ligand Non-...	4.71561	Hydrophobic	Pi-Pi T-shaped	A:HIS22	Pi-Orbitals	d:RES1	Pi-Orbitals
4	d:RES1 - A:LYS17	Yes		Ligand Non-...	5.13848	Hydrophobic	Pi-Alkyl	d:RES1	Pi-Orbitals	A:LYS17	Alkyl
5	d:RES1 - A:LYS17	Yes		Ligand Non-...	4.60945	Hydrophobic	Pi-Alkyl	d:RES1	Pi-Orbitals	A:LYS17	Alkyl
6	d:RES1 - A:ALA24	Yes		Ligand Non-...	4.2816	Hydrophobic	Pi-Alkyl	d:RES1	Pi-Orbitals	A:ALA24	Alkyl
7	d:RES1 - A:ALA24	Yes		Ligand Non-...	3.27704	Hydrophobic	Pi-Alkyl	d:RES1	Pi-Orbitals	A:ALA24	Alkyl

Figure S22: Interaction parameters between complex and peptide

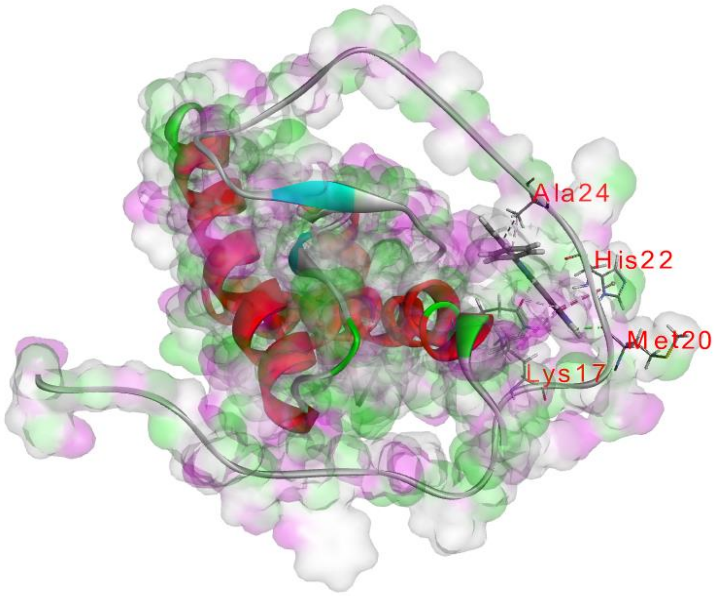

Figure S23: Hydrogen bond Donor/acceptor surface plot of peptide and complex

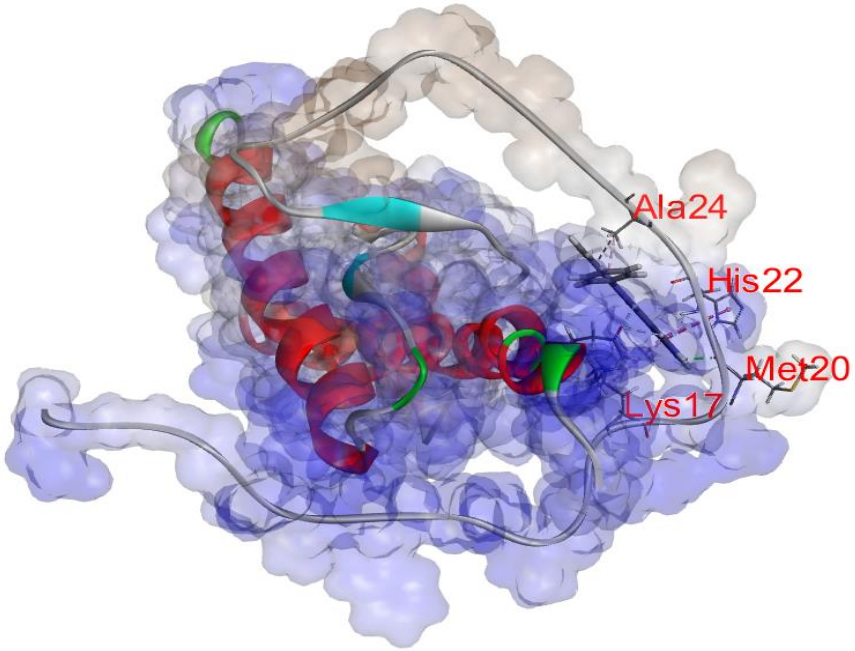

Figure S24: Hydrophobic surface plot of peptide and complex.

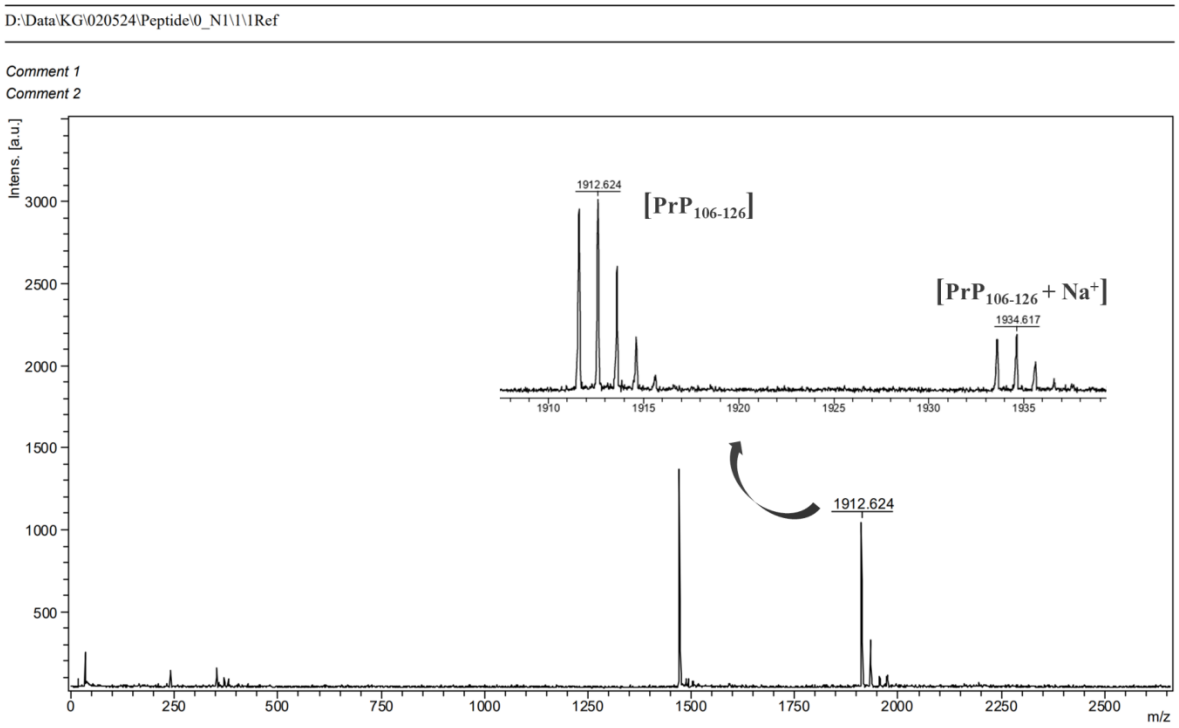

Figure S25: MALDI-TOF MS spectra of $PrP_{106-126}$

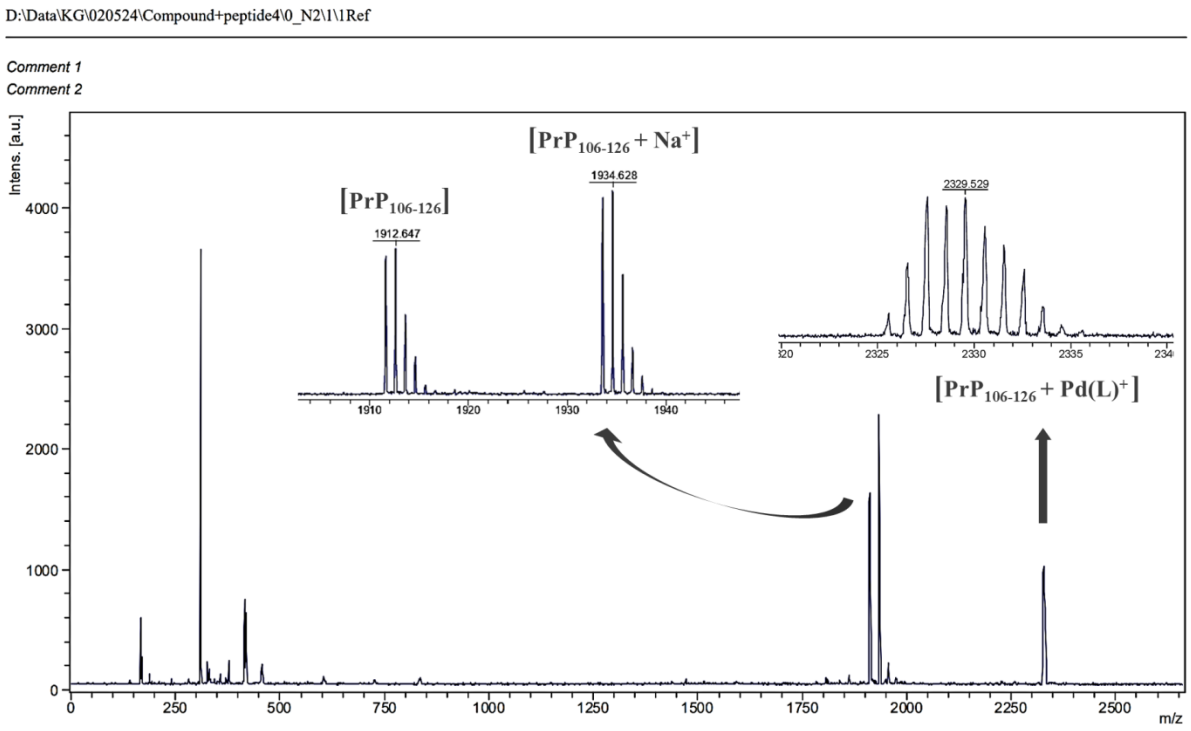

Figure S26: MALDI-TOF MS spectra of $PrP_{106-126}$ incubated with complex

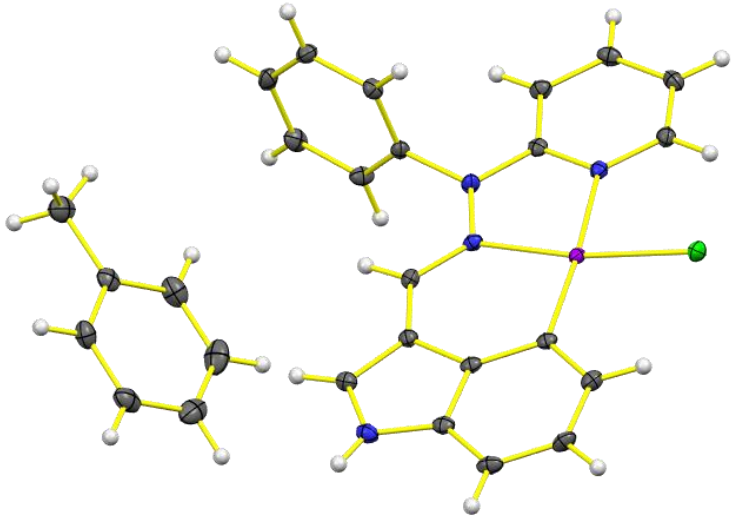

Figure S27: ORTEP plot of complex with hydrogen atoms and solvent molecule with 50% probability level.

Table S1 Crystal data and structure refinement for complex

Empirical formula	$C_{27}H_{23}ClN_4Pd$
Formula weight	545.34
Temperature/K	80.0
Crystal system	monoclinic
Space group	$P2_1/n$
a/Å	15.4895(3)
b/Å	9.3366(2)
c/Å	16.3909(3)
α/°	90
β/°	106.1750(10)
γ/°	90
Volume/Å^3	2276.61(8)
Z	4
ρ_{calc}g/cm^3	1.591
μ/mm^{-1}	0.956
F(000)	1104.0
Crystal size/mm^3	0.111 × 0.068 × 0.04
Radiation	MoKα (λ = 0.71073)
2Θ range for data collection/°	4.258 to 56.596
Index ranges	$-20 \leq h \leq 20, -12 \leq k \leq 12, -21 \leq l \leq 21$
Reflections collected	81204
Independent reflections	5661 [R_{int} = 0.0593, R_{sigma} = 0.0245]
Data/restraints/parameters	5661/0/302
Goodness-of-fit on F^2	1.069
Final R indexes [I>=2σ (I)]	R_1 = 0.0232, wR_2 = 0.0544
Final R indexes [all data]	R_1 = 0.0268, wR_2 = 0.0564
Largest diff. peak/hole / e Å^{-3}	0.56/-0.40

Table S2 Bond Lengths for complex.

Atom	Atom	Length/Å	Atom	Atom	Length/Å
Pd1	Cl1	2.3049(4)	C7	C8	1.382(2)
Pd1	N2	2.0390(14)	C7	C14	1.422(2)
Pd1	N4	2.0906(14)	C9	C13	1.405(2)
Pd1	C1	2.0023(16)	C10	C11	1.370(2)
N1	C3	1.385(2)	C11	C12	1.394(2)
N1	C8	1.356(2)	C12	C13	1.375(2)
N2	N3	1.4090(18)	C15	C16	1.389(2)
N2	C14	1.301(2)	C15	C20	1.389(2)
N3	C9	1.381(2)	C16	C17	1.388(2)
N3	C15	1.437(2)	C17	C18	1.386(2)
N4	C9	1.339(2)	C18	C19	1.383(3)
N4	C10	1.354(2)	C19	C20	1.385(2)
C1	C2	1.405(2)	C21	C22	1.390(3)
C1	C6	1.397(2)	C21	C26	1.384(3)
C2	C3	1.411(2)	C21	C27	1.504(3)
C2	C7	1.436(2)	C22	C23	1.381(3)
C3	C4	1.392(2)	C23	C24	1.379(3)
C4	C5	1.381(3)	C24	C25	1.379(3)
C5	C6	1.407(2)	C25	C26	1.388(3)

Table S3 Bond Angles for complex

Atom	Atom	Atom	Angle/°	Atom	Atom	Atom	Angle/°
N2	Pd1	Cl1	171.27(4)	C8	C7	C2	107.20(14)
N2	Pd1	N4	79.22(5)	C8	C7	C14	126.93(15)
N4	Pd1	Cl1	93.47(4)	C14	C7	C2	125.86(15)
C1	Pd1	Cl1	92.32(5)	N1	C8	C7	109.31(15)
C1	Pd1	N2	95.15(6)	N3	C9	C13	120.65(15)
C1	Pd1	N4	173.93(6)	N4	C9	N3	117.00(14)
C8	N1	C3	109.60(14)	N4	C9	C13	122.34(15)
N3	N2	Pd1	112.71(10)	N4	C10	C11	122.53(16)
C14	N2	Pd1	129.61(11)	C10	C11	C12	118.68(16)
C14	N2	N3	117.68(13)	C13	C12	C11	119.88(16)
N2	N3	C15	120.74(13)	C12	C13	C9	118.04(16)
C9	N3	N2	117.16(13)	N2	C14	C7	120.71(15)
C9	N3	C15	119.97(13)	C16	C15	N3	119.03(15)
C9	N4	Pd1	113.80(11)	C20	C15	N3	119.85(15)

C9	N4	C10	118.51(14)	C20	C15	C16	121.07(15)
C10	N4	Pd1	127.68(11)	C17	C16	C15	119.21(15)
C2	C1	Pd1	116.98(12)	C18	C17	C16	120.22(16)
C6	C1	Pd1	127.83(13)	C19	C18	C17	119.88(16)
C6	C1	C2	115.19(15)	C18	C19	C20	120.80(16)
C1	C2	C3	122.09(15)	C19	C20	C15	118.82(16)
C1	C2	C7	131.66(15)	C22	C21	C27	120.59(17)
C3	C2	C7	106.25(14)	C26	C21	C22	117.52(18)
N1	C3	C2	107.63(15)	C26	C21	C27	121.89(18)
N1	C3	C4	130.50(16)	C23	C22	C21	121.64(18)
C4	C3	C2	121.87(16)	C24	C23	C22	119.93(19)
C5	C4	C3	116.18(16)	C25	C24	C23	119.51(19)
C4	C5	C6	122.40(16)	C24	C25	C26	120.10(19)
C1	C6	C5	122.25(16)	C21	C26	C25	121.29(19)